

Research article

Tianci Feng, Xiaohui Li*, Penglai Guo, Ying Zhang, Jishu Liu and Han Zhang*

MXene: two dimensional inorganic compounds, for generation of bound state soliton pulses in nonlinear optical system

<https://doi.org/10.1515/nanoph-2020-0011>

Received January 9, 2020; accepted April 20, 2020

Abstract: MXene are a class of metal carbide and metal nitride materials with a two-dimensional layered structure. MXene $\text{Ti}_3\text{C}_2\text{T}_x$ has the characteristics of good metal conductivity and adjustable chemical composition, which has attracted the attention of scientists. Recently, MXene have shown strong nonlinear photonics and optoelectronic effect, which can be used to generate ultrashort pulsed laser. However, soliton molecules pulse in laser cavity based on MXene have not been reported at present. In this article, MXene have been characterized systematically, and the nonlinear optical characters were measured. In addition, we combined MXene with taper fiber to make a saturable absorber device for an erbium-doped fiber laser. The modulation depth and saturation absorption intensity of MXene are 10.3% and 197.5 MW/cm^2 , respectively. Thanks to the outstanding character of MXene, a three-order soliton molecules pulse were generated in laser cavity. The center wavelength, pulse interval and spectral modulation period of soliton molecules are 1529.4 nm, 15.5 ps and 0.5 nm, respectively. The above experimental results show that MXene have broad application prospects in the fields of optical fiber communication, laser material processing and high-resolution optics.

Keywords: Er-doped fiber laser; MXene; nonlinear optics; soliton molecules pulse; 2D materials.

1 Introduction

At present, with the rapid development of information technology, the demand for photoelectric functional materials grows with each passing day [1–5]. In recent years, many studies have been implemented on preparation and application of crystal nonlinear optics materials due to their excellent physical and optoelectronic properties [6–8]. Among them, scientists are particularly interested in study of two-dimensional (2D) materials [9–14]. Meanwhile, pulsed fiber laser based on 2D materials have rapid progress. In 2009, the 2D materials (i. e., graphene) were applied for mode-locked fiber lasers. Driven by graphene research, the application of 2D layered materials has developed rapidly [15]. Recently, the new 2D materials, graphene [13, 16–18], MoS_2 [19], topological insulator [20], transition metal dichalcogenides [21, 22], black phosphorus (BP) [23] and so on, have been extensively studied. MXene materials, firstly assembled in 2012 by Y. Gogotsi et al., are a class of metal carbide and metal nitride materials with a 2D layered structure [24]. The general formula of MXene is $\text{M}_{n+1}\text{X}_n\text{T}_x$ ($n = 1, 2, 3$). In this formula, M is a transition metal element, and X is carbon element (C) or nitrogen element (N), and T represents a surface end group (Such as $-\text{O}$, $-\text{OH}$, or $-\text{F}$ and so on). MXene was obtained by etching method which using hydrofluoric solution etching the A atom layer of MAX phase material. Here, A is the elements of group IIIA or IVA [25–27]. Density functional theoretical result shows that $\text{Ti}_3\text{C}_2\text{T}_x$ not only can be stably present, but also have good metallicity. The average band gap of MXene is smaller than 0.2 eV, which indicates that MXene can be potentially used in mode-locked fiber laser as saturable absorber (SA).

Fiber laser is a kind of new generation solid-state laser, which has the advantages of high photoelectric conversion efficiency, high stability, and good beam quality [28–31]. At present, fiber laser have become the mainstream of laser technology development. In many applications, pulsed fiber lasers have been studied extensively because they provide high power density. Due to different dispersion of fiber lasers, a large number of

*Corresponding authors: Xiaohui Li, School of Physics & Information Technology, Shaanxi Normal University, Xian, 710119, PR China, E-mail: lixiaohui0523@163.com; and Han Zhang, Shenzhen Key Laboratory of Two-Dimensional Materials and Devices/Shenzhen Engineering Laboratory of Phosphorene and Optoelectronics, Collaborative Innovation Center for Optoelectronic Science and Technology, Key Laboratory of Optoelectronic Devices and Systems of Ministry of Education and Guangdong, Shenzhen, 518060, PR China, E-mail: hzhang@szu.edu.cn. <https://orcid.org/0000-0002-5600-3820>
Tianci Feng, Penglai Guo, Ying Zhang and Jishu Liu: School of Physics & Information Technology, Shaanxi Normal University, Xian, 710119, PR China

experimental and theoretical results show that the output pulse characteristics of fiber lasers are various. The output pulse can be divided into conventional solitons (CSs), self-similar pulses, soliton molecules, dissipative solitons, and dissipative soliton resonant etc. [32–37]. Among them, multiple solitons pulse can form bound solitons through interaction. When the two sub-pulses are close together, they will repel each other. On the contrary, when the two sub-pulses are far apart, they attract each other and finally reach the equilibrium distance. This phenomenon can also be called soliton molecules pulse because it is similar to a chemical molecule [38–41]. MXene as a novel 2D material has been investigated recently. In 2017, MXene was used in erbium-doped fiber laser (EDFL) to achieve mode-locked pulsed laser output [42]. In 2018, the optical nonlinear absorption characteristics of MXene were measured at 800~1800 nm range [24]. In 2019, the EDFL based on MXene achieved high-power pulsed laser output with an average power of 40 mW [43]. However, soliton molecules pulse in laser cavity based on MXene have not been reported at present.

In this work, the optical characteristics as well as application of MXene in pulsed fiber laser have been systematically studied. The sample has a wide absorption range in ultraviolet visible infrared absorption spectrum. In addition, the microfiber with low loss is prepared by the melting method. MXene is deposited on tapered area of microfiber as a SA device to apply a mode-locked fiber laser. We built an optical nonlinear measurement system for SA. The modulation depth and saturation absorption intensity are 10.3% and 197.5 MW/cm², respectively. CSs with 980-fs pulse width and three-order soliton molecules pulse with 15.5 ps pulse interval are obtained under certain pump power and polarization orientation, respectively. The experimental results show that MXene has broad application prospects in the fields of optical fiber communication, laser material processing and high-resolution optics.

2 Preparation and characterization of MXene

At present, the synthetic methods of MXene mainly are solution method (HF and HCl + LiF), high-temperature fluoride melting method and the bottom-up synthesis method. Among them, HF etching MAX has certain advantages compared with the other two methods such as low cost, high practicability and mature synthesis process. Here, as show in Figure 1(a), we used the etching

method to obtain the 2D layered material MXene. First, a small amount of Ti₃AlC₂ powder is grinded. Secondly, the ground Ti₃AlC₂ powder was slowly added to HF solution and stirred. Finally, after 60 h, the reaction liquid is put into the test tube, and the MXene was centrifugally cleaned until the pH of solution reached neutrality. After centrifugation, the reaction liquid is put into the vacuum drying box and dried. The phase of MAX is a hexagonal layered structure where the X atoms are filled in the octahedral spaces formed by the M atoms. As shown in Figure 1(b), the MX layer and the A atomic layer are alternately arrange. There are synthesized more than 70 types of MAX currently. In the MAX phase, there is a strong covalent bond between M and X, and a relatively weak metal bond between M and A. The etching of Ti₃AlC₂ is selective, which the Ti–Al bond with a weak bond energy is preferentially selected. So, the Ti–C layer connected by the Al atom layer is separated. This method is similar to the preparation of graphene by the Hummer method, which requires overcoming the van der Waals force between the layers of graphite. To emphasize its similar properties to graphene, it is named MXene. Figure 1(c) is the prepared MXene dispersion liquid. In order to find out the structure of Ti₃C₂T_x, it is characterized by Scanning Electron Microscope (SEM, Product Code: Nova nanoSEM 450). As shown in Figure 1(d) and 1(e), the 2D structure of the Ti₃C₂T_x layer is clearly visible. As show in Figure 1(f), the size of sample is 108.7 nm, which is measured by High Resolution Transmission Electron Microscopy (HRTEM, Product Code: Tecnai G2 F20). Figure 1(g) shows the HRTEM with the 10 nm scale. The space group of MXene is P6₃/mmc. The atomic layers structure of Ti₃C₂T_x is shown in Figure 1(h). As shown in Figure 1(i), the component of sample is analyzed by Energy Dispersive Spectroscopy (EDS, Product Code: XRF-1800). Among them, Al element is caused by the table of measuring instrument, and the Si element is caused by the substrate where the sample is located. In this figure, the rate of sample element mass is clearly visible. The ultraviolet visible infrared absorption spectrum of MXene can be seen in Figure 1(j), which indictes that the sample has a wide absorption range in this band. In this curve, the linear absorption of the sample is 3.92% at 1530 nm. The absorption line has a large fluctuation at 800 nm due to the absorption of water and carbon dioxide in the air when the instrument is replaced light source. The absorption spectrum of the sample in the ultraviolet-visible-infrared (UV–vis-IR, Product Code: Lambda 1050) band indicates that it can be applied to the laser generation at 1530 nm. As shown in Figure 1(k), The Raman spectra were recorded using a Raman spectrometer

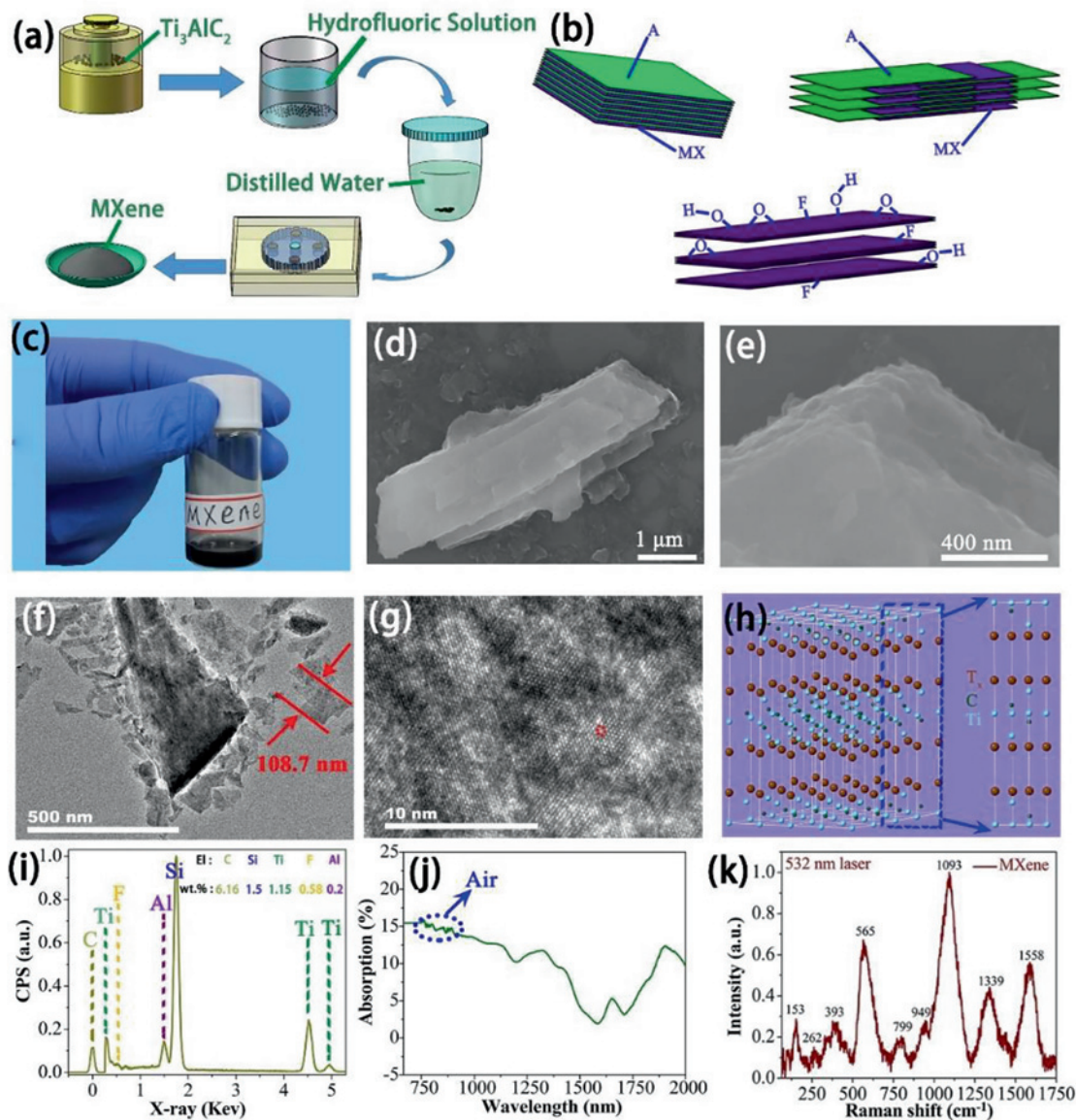


Figure 1: (a) Preparation of MXene flow chart. (b) Schematic of the exfoliation process for Ti_3AlC_2 . (c) Photograph of the MXene dispersion liquid. (d) SEM image with scale of 1 μm . (e) SEM image with scale of 400 nm. (f) TEM image with 500 nm. (g) HRTEM image with 10 nm. (h) The atomic layers' structure of MXene. (i) EDS spectrum. (j) Absorption spectrum. (k) Raman spectrum.

(Product Code: LabRAM HR Evolution) with 532 nm as the excitation laser. The peaks at 393 and 565 cm^{-1} are attributed to the O atoms E_g and A_{1g} vibrations, respectively. The peak at 262 cm^{-1} is occurs due to the contribution of H atoms vibration in the $\text{Ti}_3\text{C}_2\text{T}_x$. The vibration of Ti-C and C-C bonds cause the appearance of peak at 797 cm^{-1} [44]. In addition, the D (A_{1g}) and G (E_{2g}) bands of disordered carbon cause the appearance of 1339 and 1558 cm^{-1} peaks, respectively [45]. The ω_1 (E_g) Raman active phonon vibration mode corresponds to the peak of 153 cm^{-1} [46]. These section may be from Ti_3AlC_2 which has not been completely etched.

3 Fabrication and nonlinear absorption of SA

Optical fiber integration methods mainly include fiber end-face optical deposition, 2D materials-polymer materials composite films, microfiber optical deposition, side-draw D-shaped optical fiber deposition, photonic crystal fiber perfusion, etc. Among them, microfiber has many excellent optical transmission characteristics such as strong evanescent field, extremely high damage threshold and small mass compared with other methods.

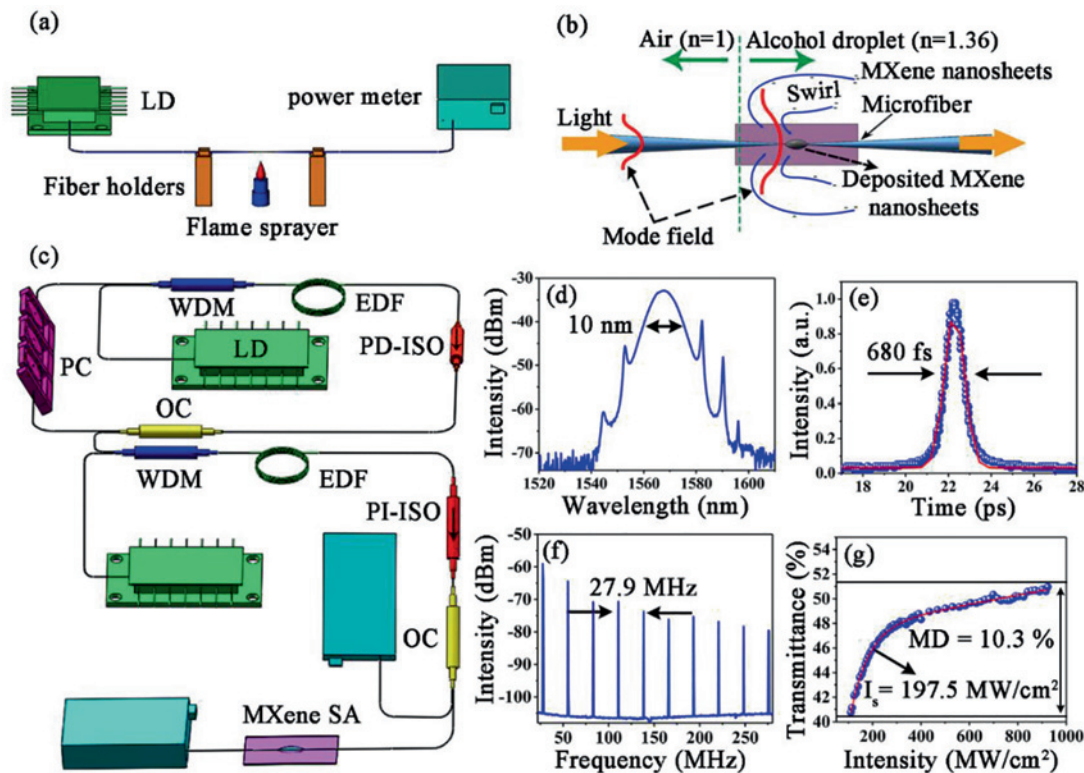


Figure 2: (a) Experimental setup for fabricating of microfiber. (b) Schematic of optical deposition. (c) Detector system of the nonlinear absorbance. (d) Output spectrum of seed light. (e) Autocorrelation map of seed light pulse. (f) Radio frequency spectrum of seed light pulse. (g) Nonlinear transmittance curve (the blue and red curves represent the experimental and fitting results respectively).

As shown in Figure 2(a), a single mode fiber (SMF-28) with a length of 60 cm is intercepted. The optical fiber is heated to the molten state on the flame. Meanwhile, the two sides of the optical fiber are stretched at a certain speed, which eventually form the microfiber. The tapered area length and minimum diameter of the microfiber is about 0.8 cm and 18 μm , respectively. The loss of the microfiber is measured to be 51%. When we connect the device into the ring cavity, the change of power is within the allowable error range. Among them, the error is caused by welding loss. As shown in Figure 2(b), a few MXene dispersion liquid is dropped on the tapered region of microfiber. The deposition principle is that light causes swirl and convection in alcohol. We use a power meter to observe how much material has been deposited. The advantage of this method is that the deposition only occurs at the boundary of the incident light, which allows us to selectively deposit the solution to a specified area. The transmittance characteristics of MXene can be measured by power related method. Figure 2(c) is the measurement system of nonlinear absorbance. A nonlinear polarization rotation mode-locked pulse laser was built. Among them, the pump source uses a company II-VI's laser diode (LD) with a

central wavelength of 974 nm (Product Code: CM96Z400-74). The nonlinear optical parameters of SA are highly dependent on the excitation conditions. The output characteristics of the seed lasers are shown in Figure 2 (d) and (e). The center wavelength, 3-dB spectral width and pulse duration are 1569 nm, 10 nm and 680 fs, respectively. Figure 2(f) shows the radio frequency spectrum in window of 250 MHz, which has a good stability due to the fluctuation of the spectral line is small.

The mathematical model of the nonlinear measurement system as follows:

$$T = 1 - \frac{\alpha_0}{1 + \frac{I}{I_s}} - \alpha_{ns}, \quad (1)$$

where α_0 is the linear parameter of saturable absorption, I is the input intensity, α_{ns} is the non-saturation absorption intensity, and I_s is the saturation absorption intensity. Figure 2(g) shows that the MXene SA has a modulation depth of 10.3% and a non-saturation absorbance of 49.1%, which is sufficient to modulate the laser to achieve mode-locked pulse output. The saturation absorption intensity is 197.5 MW/cm^2 . In addition, as shown in the following Table 1, we compare the saturable absorption characteristics

Table 1: The comparison of optical nonlinearity based on MXene SA devices under various experimental conditions [43, 44, 47–49].

| MXene | EP | λ_c (nm) | I_{sat} (MW/ cm ²) | MD (%) | NSA (%) | Refs |
|---|----------------|------------------|--|-----------|------------|-----------|
| Ti ₃ C ₂ T _x | QS | 1560 | 191 | 2.8 | 59.7 | 43 |
| | HM | 1566.9 | 256.9 | 0.96 | 73.5 | 44 |
| | CSs | 1560 | 7.3 | 41 | 2 | 47 |
| | CSs | 1558 | — | 11.3 | 1 | 48 |
| Ti ₂ CT _x | QS and CSs | 1560 | 5.1 | 15.7 | 21 | 49 |
| Ti ₃ C ₂ T _x | Soliton | 1569 | 197.5 | 10.3 | 49.1 | This work |
| | Mole- cules | | | | | |

λ_c , Center wavelength; EP, Experimental phenomena; MD, Modulation depth; NSA, Non-saturation absorbance; QS: Q-Switching; HM, Harmonic mode-locking.

of MXene SA with the previous work. The data show that MXene can be used as a good saturable absorber in mode-locked fiber laser to generate soliton molecules.

4 The experimental results and discussions

Figure 3(a) shows that the pump source uses a company II-VI's laser diode (LD) with a central wavelength of 974 nm (Product Code: CM96Z400-74). The light is combined into a bundle by a 980/1550 nm wavelength division multiplexer (WDM). As a gain medium, the EDF (model number: EDF-4/125-50) length, the peak absorption at 1530 nm and dispersion parameters are 1.02 m, 50 dB/m and -36 ps/(nm·km), respectively. The remaining fibers are all standard SMF with dispersion parameter of 17 ps/(nm·km). The total length of the ring cavity is approximately 17.2 m, and net dispersion of the cavity is -0.136 ps². The polarization-independent isolator (PI-ISO) is used to ensure the unidirectional operation of the light in the ring cavity and improve the signal-to-noise ratio (SNR) of the output laser. The change in intracavity loss and polarization state is achieved by depositing MXene material on the microfiber, where MXene acts as a SA in the laser cavity. The laser passes through a fiber coupler with a coupling ratio of 50.3:49.7. Among them, 50.3% of the optical intensity is used to circulate and amplify in the cavity, and 49.7% is used as the output of the laser to measure the spectrum, pulse sequence, frequency, SNR and time-delay waveform of the output pulses. The measurement instruments are optical spectrum analyzer (OSA, Anritsu MS9710C), photoelectric detector (Thorlabs DET01CFC), oscilloscope

(Rigol DS6104), radio frequency spectrum analyzer (Rohde & Schwarz FSC6) and autocorrelator (Femtochrome FR-103XL, Res = 5 fs).

First, we measurement the optical output characteristics of laser cavity without MXene SA, which comes to the conclusions that the mode-locking phenomenon never come. After plugging the MXene SA in cavity, the broaden spectrum and stable pulse sequence can be observed when the pump power is 260 mW. In general, in the negative dispersion fiber laser, dispersion will lead to the collapse of optical transmission, and nonlinearity will lead to the convergence of optical transmission. Optical solitons are produced when the nonlinearity and dispersion are balanced in the laser cavity. As shown in Figure 3(b), the mode-locked pulse sequence has a time interval of 83 ns, which corresponds to one cycle of the optical pulse operation in the cavity. Figure 3(c) is the spectrum of the mode-locking. The central wavelength of the output spectrum is 1530.4 nm, and the 3-dB spectral width is 2.7 nm. Figure 3(d) is a pulse curve measured at pump power of 297 mW. The pulse width is 980 fs with Gaussian fitting. The time-bandwidth product of the output pulse is about 0.74, which is close to the transform limited value (0.315). The result shows that there is less chirp in the cavity. Figure 3(e) is radio frequency (RF) spectrum, which can be seen that the repetition frequency of the output pulse is 12.037 MHz. It has been proved in theory and experiment that the soliton will split with the increase of pump power. The traditional soliton mode-locked fiber laser is affected by the theory of soliton area, and its pulse width and energy are limited. When the pump power in the cavity is too high, the soliton pulse will split [50]. As shown in Figure 3(f), the pulses are split as the pump power increase. Figure 3(g) indicates the result that the output power and pulse energy changing with pump power. When the forces between the split solitons are balanced, a stable soliton molecule is formed. Through changing the pump power and adjusting the polarization controller, a stable three-order soliton molecules pulse is obtained at pump power of 356.2 mW. Figure 3(h) shows the three-order soliton molecule pulse spectrum, which the phase difference is 0 between the two adjacent solitons. It is not difficult to find that there is significant periodic modulation on the spectrum due to the interference between the two pulses. The modulation period is 0.5 nm. The central wavelength of the soliton molecule pulse is 1529.4 nm. Figure 3(i) is the autocorrelation curve, which intensity ratio of five peaks is 1:2:3:2:1. The pulse width and duration of the pulse are 870 fs and 15.5 ps, respectively. The corresponding ratio is

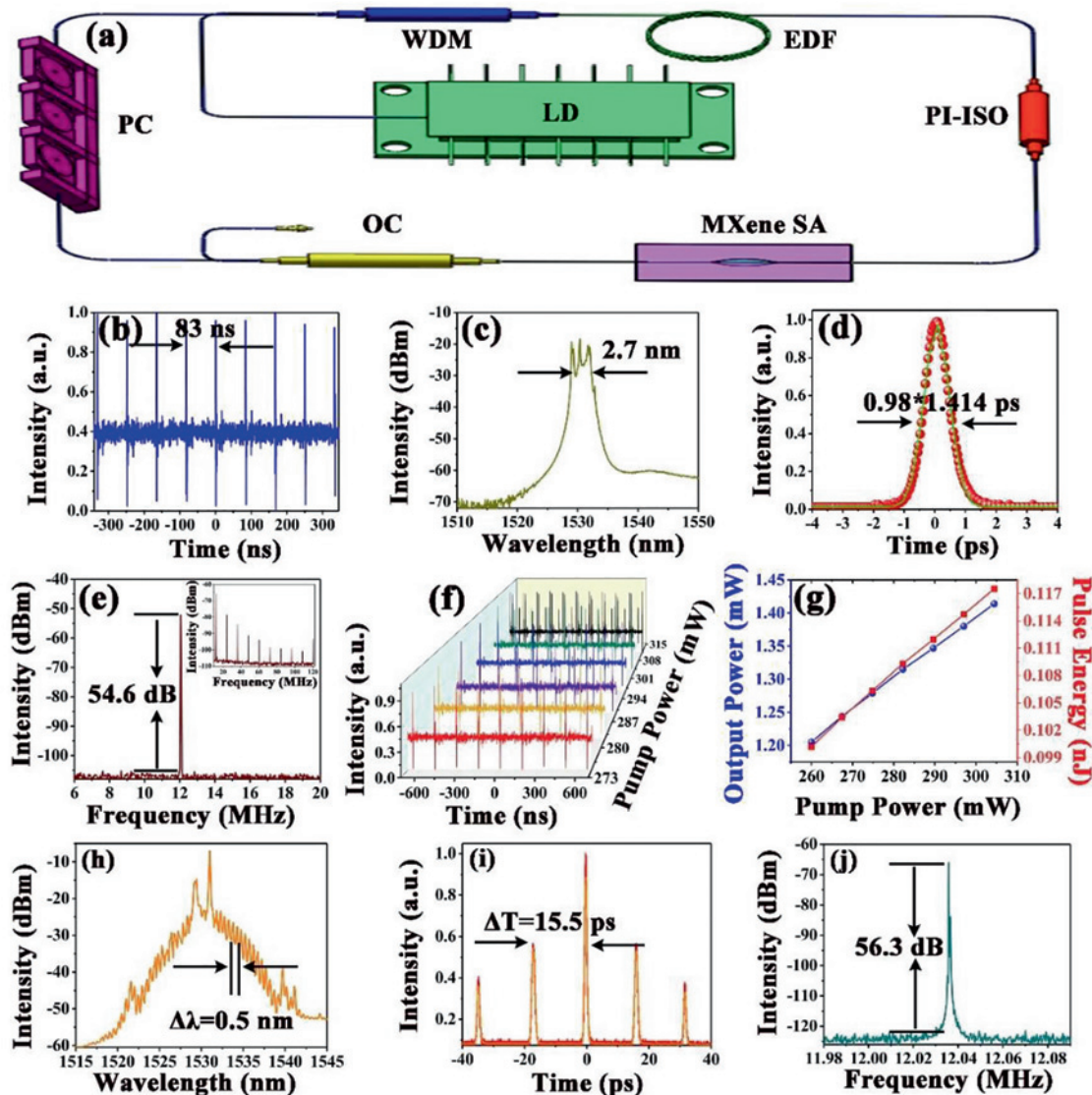


Figure 3: (a) Schematic of mode-locked fiber laser. (b) Typical oscilloscope pulse trains of mode-locking. (c) Mode-locked optical spectrum. (d) Autocorrelation trace with a gauss fitting (the red and green curves represent the experimental and fitting results respectively). (e) Frequency spectrum of the output pulse. (f) Pulse evolution. (g) Output power and pulse energy changing results with pump power. (h) spectrum of soliton molecule pulse. (i) Autocorrelation curve of soliton molecule pulse. (j) Frequency spectrum of soliton molecule pulse.

1:17.8. According to the Fourier transform, the spectral modulation $\Delta\lambda$ and the sub-pulse time interval ΔT satisfy the following relationship:

$$\Delta T = \left| \frac{\lambda_0^2}{c \cdot \Delta\lambda} \right| \quad (2)$$

In this formula, λ_0 is the central wavelength of the pulse spectrum, and c represents the speed of the light in the vacuum. Figure 3(j) is an RF spectrum, which can be seen that the SNR is 56.3 dB.

In this experiment, we can see that there is no Kelly sidebands in the CS spectrum in Figure 3 because the

output signal of the laser cavity is weak. Thus, we added a laser amplifier behind the laser cavity to measure the autocorrelation data. The added optical path outside the laser cavity will not distort the output signal. Table 2 shows a comparison of the output laser characteristics of MXene and other materials after their application in fiber lasers. Mxene is similar to graphene in near zero band gap optical properties, and is expected to replace graphene as a novel 2D material with widely application in the future. It can be seen from the absorption curve that MXene has a high optical transmittance. In addition, the modulation depth and saturation intensity of saturable device are 10.3% and

Table 2: The comparison of the output laser characteristics in resonators based on different SA devices [51–54].

| Materials | Band gap (eV) | MD (%) | I_s (MW/cm ²) | λ_c (nm) | 3-dB bandwidth (nm) | Pulse duration (fs) | SNR (dB) | ref |
|---------------------------------|---------------|--------|-----------------------------|------------------|---------------------|---------------------|----------|-----------|
| Graphene | 0 | 65.9 | 0.53 | 1561 | 5 | 1230 | 60 | 51 |
| Bi ₂ Te ₃ | 0.33 | 2 | 180 | 1557 | 2.9 | 1100 | 75 | 52 |
| MoSe ₂ | 1.46 | 0.63 | 19.8 | 1558 | 1.76 | 1760 | 61.5 | 53 |
| BP | 1.15 | 8.1 | 6.55 | 1571.4 | 2.9 | 946 | 70 | 54 |
| MXene | 0.2 | 10.3 | 197.5 | 1530.4 | 2.7 | 980 | 54.6 | This work |

197.5 MW/cm², respectively, which means MXene can be used as saturable absorber in fiber laser. The experimental results show that MXene are excellent material in the application of ultrashort pulse generation.

5 Conclusions

In this paper, MXene are deposited on microfiber as SA to Er-doped fiber lasers obtaining CSs and there-order soliton molecules output. When the pump power is 260 mW, CSs appear in the laser cavity. The spectral central wavelength of CSs is 1530.4 nm, and the 3-dB spectral width is 2.7 nm. The time interval between the two pulses is 83 ns. The cavity length, the repetition rate and the SNR are 17.2 m, 12.037 MHz and 54.6 dB, respectively. The pulse width is 980 fs with Gauss fitting. The TBP of the output pulse is about 0.74, which indicates that there is less chirp in the cavity. With the change of power and polarization controller, we obtain a three-order soliton molecules pulse with phase difference of 0. The results show that MXene can be used as SA to study soliton molecules in Er-doped fiber laser. Compared with the typical 2D materials such as graphene and MoS₂, MXenes not only has large specific surface area, but also has good metal conductivity, adjustable chemical composition advantages. Furthermore, MXene has wide application prospects in the fields of optical fiber communication, laser material processing and high-resolution optics [55, 56].

Acknowledgment: This research was supported by the National Natural Science Foundation of China (grant number 61605106); Fundamental Research Funds for the Central Universities (GK201802006); Open Research Fund of State Key Laboratory of Transient Optics and Photonics, Chinese Academy of Sciences (number SKLST201809); Starting Grants of Shaanxi Normal University (grant number 1112010209, 1110010717).

Conflict of interest: The authors declare no conflicts of interest.

References

- [1] X. C. Yu, Y. Y. Li, X. N. Hu, et al., “Narrow bandgap oxide nanoparticles coupled with graphene for high performance mid-infrared photodetection,” *Nat. Commun.*, vol. 9, p. 8, 2018. <https://doi.org/10.1038/s41467-018-06776-z>.
- [2] Y. Song, Z. Liang, X. Jiang, et al., “Few-layer antimonene decorated microfiber: ultra-short pulse generation and all-optical thresholding with enhanced long term stability,” *2D Mater.*, vol. 4, 2017. <https://doi.org/10.1088/2053-1583/aa87c1>.
- [3] J. Jiang, W. Hu, D. Xie, et al., “2D electric-double-layer phototransistor for photoelectronic and spatiotemporal hybrid neuromorphic integration,” *Nanoscale*, vol. 11, pp. 1360–1369, 2019. <https://doi.org/10.1039/C8NR07133K>.
- [4] J. Li, Z. L. Zhang, J. Yi, et al., “Broadband spatial self-phase modulation and ultrafast response of MXene Ti₃C₂T_x (T=O, OH or F),” *Nanophotonics*, 2020. <https://doi.org/10.1515/nanoph-2019-0469>.
- [5] C. Wang, Y. Z. Wang, X. T. Jiang, et al., “MXene Ti₃C₂T_x: a promising photothermal conversion material and application in all-optical modulation and all-optical information loading,” *Adv. Opt. Mater.*, vol. 7, 2019, Art no. 1900060. <https://doi.org/10.1002/adom.201900060>.
- [6] N. N. Xu, P. F. Ma, S. G. Fu, et al., “Tellurene-based saturable absorber to demonstrate large-energy dissipative soliton and noise-like pulse generations,” *Nanophotonics*, 2020. <https://doi.org/10.1515/nanoph-2019-0545>.
- [7] J. Guo, J. L. Zhao, D. Z. Huang, et al., “Two-dimensional tellurium-polymer membrane for ultrafast photonics,” *Nanoscale*, vol. 11, pp. 6235–6242, 2019. <https://doi.org/10.1039/c9nr00736a>.
- [8] N. Ming, S. N. Tao, W. Q. Yang, et al., “Mode-locked Er-doped fiber laser based on PbS/CdS core/shell quantum dots as saturable absorber,” *Opt Express*, vol. 26, pp. 9017–9026, 2018. <https://doi.org/10.1364/OE.26.009017>.
- [9] Q. Q. Yang, R. T. Liu, C. Huang, et al., “2D bismuthene fabricated via acid-intercalated exfoliation showing strong nonlinear near-infrared responses for mode-locking lasers,” *Nanoscale*, vol. 10, pp. 21106–21115, 2018. <https://doi.org/10.1039/c8nr06797j>.
- [10] Y. Q. Ge, Z. F. Zhu, Y. H. Xu, et al., “Broadband nonlinear photoresponse of 2D TiS₂ for ultrashort pulse generation and all-optical thresholding devices,” *Adv. Opt. Mater.*, vol. 6, p. 10, 2018. <https://doi.org/10.1002/adom.201701166>.
- [11] K. D. Niu, R. Y. Sun, Q. Y. Chen, B. Y. Man, and H. N. Zhang, “Passively mode-locked Er-doped fiber laser based on SnS₂ nanosheets as a saturable absorber,” *Photonics Res.*, vol. 6, pp. 72–76, 2018. <https://doi.org/10.1364/PRJ.6.000072>.

- [12] L. Lu, Z. M. Liang, L. M. Wu, et al., “Few-layer bismuthene: sonochemical exfoliation, nonlinear optics and applications for ultrafast photonics with enhanced stability,” *Laser Photon. Rev.*, vol. 12, p. 10, 2018. <https://doi.org/10.1002/lpor.201700221>.
- [13] H. Zhang, D. Y. Tang, R. J. Knize, L. M. Zhao, Q. L. Bao, and K. P. Loh, “Graphene mode locked, wavelength-tunable, dissipative soliton fiber laser,” *Appl. Phys. Lett.*, vol. 96, p. 3, 2010. <https://doi.org/10.1063/1.3367743>.
- [14] X. Yu, P. Yu, D. Wu, et al., “Atomically thin noble metal dichalcogenide: a broadband mid-infrared semiconductor,” *Nat Commun.*, vol. 9, p. 1545, 2018. <https://doi.org/10.1038/s41467-018-03935-0>.
- [15] B. Fu, J. Li, Z. Cao, and D. Popa, “Bound states of solitons in a harmonic graphene-mode-locked fiber laser,” *Photonics Res.*, vol. 7, 2019. <https://doi.org/10.1364/PRJ.7.000116>.
- [16] Z. P. Sun, T. Hasan, F. Torrisi, et al., “Graphene mode-locked ultrafast laser,” *ACS Nano*, vol. 4, pp. 803–810, 2010. <https://doi.org/10.1021/nn901703e>.
- [17] Z. Q. Luo, M. Zhou, J. Weng, et al., “Graphene-based passively Q-switched dual-wavelength erbium-doped fiber laser,” *Opt. Lett.*, vol. 35, pp. 3709–3711, 2010. <https://doi.org/10.1364/OL.35.003709>.
- [18] Q. L. Bao, H. Zhang, Y. Wang, et al., “Atomic-layer graphene as a saturable absorber for ultrafast pulsed lasers,” *Adv. Funct. Mater.*, vol. 19, pp. 3077–3083, 2009. <https://doi.org/10.1002/adfm.200901007>.
- [19] Z. Y. Yin, H. Li, H. Li, et al., “Single-layer MoS₂ phototransistors,” *ACS Nano*, vol. 6, pp. 74–80, 2012. <https://doi.org/10.1021/nn2024557>.
- [20] P. G. Yan, R. Y. Lin, H. Chen, et al., “Topological insulator solution filled in photonic crystal fiber for passive mode-locked fiber laser,” *IEEE Photonics Technol. Lett.*, vol. 27, pp. 264–267, 2015. <https://doi.org/10.1109/LPT.2014.2361915>.
- [21] T. Feng, D. Zhang, X. Li, et al., “SnS₂ nanosheets for Er-doped fiber lasers,” *ACS Appl. Nano Mater.*, vol. 3, pp. 674–681, 2020. <https://doi.org/10.1021/acsanm.9b02194>.
- [22] J. S. Liu, X. H. Li, Y. X. Guo, et al., “SnSe₂ nanosheets for subpicosecond harmonic mode-locked pulse generation,” *Small*, vol. 15, 2019, Art no. e1902811. <https://doi.org/10.1002/sml.201902811>.
- [23] Y. Chen, G. B. Jiang, S. Q. Chen, et al., “Mechanically exfoliated black phosphorus as a new saturable absorber for both Q-switching and mode-locking laser operation,” *Opt. Express*, vol. 23, pp. 12823–12833, 2015. <https://doi.org/10.1364/OE.23.012823>.
- [24] M. Naguib, J. Come, B. Dyatkin, et al., “MXene: a promising transition metal carbide anode for lithium-ion batteries,” *Electrochem. Commun.*, vol. 16, pp. 61–64, 2012. <https://doi.org/10.1016/j.elecom.2012.01.002>.
- [25] C. Wang, Q. Q. Peng, X. W. Fan, et al., “MXene Ti₃C₂T_x saturable absorber for pulsed laser at 1.3 μm,” *Chin. Phys. B*, vol. 27, p. 4, 2018. <https://doi.org/10.1088/1674-1056/27/9/094214>.
- [26] X. Y. Feng, B. Y. Ding, W. Y. Liang, et al., “MXene Ti₃C₂T_x absorber for a 1.06 μm passively Q-switched ceramic laser,” *Laser Phys. Lett.*, vol. 15, p. 5, 2018. <https://doi.org/10.1088/1612-202X/150505>.
- [27] H. Lin, X. G. Wang, L. D. Yu, Y. Chen, and J. L. Shi, “Two-dimensional ultrathin MXene ceramic nanosheets for photothermal conversion,” *Nano Lett.*, vol. 17, pp. 384–391, 2017. <https://doi.org/10.1021/acs.nanolett.6b04339>.
- [28] C. Dou, W. Wen, J. Wang, et al., “Ternary ReS_{2(1-x)}Se_{2x} alloy saturable absorber for passively Q-switched and mode-locked erbium-doped all-fiber lasers,” *Photonics Res.*, vol. 7, 2019. <https://doi.org/10.1364/PRJ.7.000283>.
- [29] J. J. Guo, J. Jiang, and B. C. Yang, “Low-voltage electric-double-layer MoS₂ transistor gated via water solution,” *Solid-State Electron.*, vol. 150, pp. 8–15, 2018. <https://doi.org/10.1016/j.sse.2018.10.001>.
- [30] B. Guo, S. H. Wang, Z. X. Wu, et al., “Sub-200 fs soliton mode-locked fiber laser based on bismuthene saturable absorber,” *Opt. Express*, vol. 26, pp. 22750–22760, 2018. <https://doi.org/10.1364/OE.26.022750>.
- [31] P. G. Yan, R. Y. Lin, S. C. Ruan, A. J. Liu, and H. Chen, “A 2.95 GHz, femtosecond passive harmonic mode-locked fiber laser based on evanescent field interaction with topological insulator film,” *Opt. Express*, vol. 23, pp. 154–164, 2015. <https://doi.org/10.1364/OE.23.000154>.
- [32] Y. Zhang, X. H. Li, A. Qyyum, et al., “PbS nanoparticles for ultrashort pulse generation in optical communication region,” *Part. Part. Sys. Character.*, vol. 35, p. 6, 2018. <https://doi.org/10.1002/ppsc.201800341>.
- [33] Y. X. Guo, X. H. Li, P. L. Guo, and H. R. Zheng, “Supercontinuum generation in an Er-doped figure-eight passively mode-locked fiber laser,” *Opt. Express*, vol. 26, pp. 9893–9900, 2018. <https://doi.org/10.1364/OE.26.009893>.
- [34] T. Chai, X. H. Li, T. C. Feng, et al., “Few-layer bismuthene for ultrashort pulse generation in a dissipative system based on an evanescent field,” *Nanoscale*, vol. 10, pp. 17617–17622, 2018. <https://doi.org/10.1039/C8NR03068E>.
- [35] X. Liu, D. Popa, and N. Akhmediev, “Revealing the transition dynamics from Q switching to mode locking in a soliton laser,” *Phys. Rev. Lett.*, vol. 123, 2019, Art no. 093901. <https://doi.org/10.1103/PhysRevLett.123.093901>.
- [36] X. Liu and M. Pang, “Revealing the buildup dynamics of harmonic mode-locking states in ultrafast lasers,” *Laser Photon. Rev.*, vol. 13, 2019. <https://doi.org/10.1002/lpor.201800333>.
- [37] Y. Song, X. Shi, C. Wu, D. Tang, and H. Zhang, “Recent progress of study on optical solitons in fiber lasers,” *Appl. Phys. Rev.*, vol. 6, 2019. <https://doi.org/10.1063/1.5091811>.
- [38] L. L. Gui, P. Wang, Y. H. Ding, et al., “Soliton molecules and multisoliton states in ultrafast fibre lasers: intrinsic complexes in dissipative systems,” *Appl. Sci. Basel*, vol. 8, p. 31, 2018. <https://doi.org/10.3390/app8020201>.
- [39] C. Wang, L. Wang, X. H. Li, et al., “Few-layer bismuthene for femtosecond soliton molecules generation in Er-doped fiber laser,” *Nanotechnology*, vol. 30, p. 9, 2019. <https://doi.org/10.1088/1361-6528/aae8c1>.
- [40] J. Guo, “Bound-state solitons in a linear-cavity fiber laser mode-locked by single-walled carbon nanotubes,” *J. Mod. Opt.*, vol. 61, pp. 980–985, 2014. <https://doi.org/10.1080/09500340.2014.916361>.
- [41] J. H. Lin, C. W. Chan, H. Y. Lee, and Y. H. Chen, “Bound states of dispersion-managed solitons from single-mode Yb-doped fiber laser at net-normal dispersion,” *IEEE Photonics J.*, vol. 7, p. 9, 2015. <https://doi.org/10.1109/JPHOT.2015.2481600>.
- [42] Y. I. Jhon, J. Koo, B. Anasori, et al., “Metallic MXene saturable absorber for femtosecond mode-locked lasers,” *Adv. Mater.*, vol. 29, p. 8, 2017. <https://doi.org/10.1002/adma.201702496>.
- [43] L. Wang, X. Li, C. Wang, et al., “Few-Layer Mxene Ti₃C₂T_x (T=F, O, or OH) for robust pulse generation in a compact Er-doped fiber

- laser,” *Chem. Nano Mat.*, vol. 5, pp. 1233–1238, 2019. <https://doi.org/10.1002/cnma.201900309>.
- [44] J. Feng, X. Li, T. Feng, Y. Wang, J. Liu, and H. Zhang, “An harmonic mode-locked Er-doped fiber laser by the evanescent field-based MXene $\text{Ti}_3\text{C}_2\text{T}_x$ (T=F, O, or OH) saturable absorber,” *Anal. der Physik*, 2019, vol. 532, p. 1900437. <https://doi.org/10.1364/oe.26.031244>.
- [45] H. Ahmad, H. S. M. Albaqawi, N. Yusoff, W. Y. Chong, M. Yasin, “Q-switched fiber laser at 1.5 μm region using Ti_3AlC_2 MAX phase-based saturable absorber,” *IEEE J. Quantum Electron.*, vol. 56, p. 1600106, 2020. <https://doi.org/10.1109/JQE.2019.2949798>.
- [46] T. Hu, J. M. Wang, H. Zhang, Z. J. Li, M. M. Hu, X. H. Wang, “Vibrational properties of Ti_3C_2 and $\text{Ti}_3\text{C}_2\text{T}_2$ (T = O, F, OH) monosheets by first-principles calculations: a comparative study,” *Phy. Chem. Chem. Phys.*, vol. 17, pp. 9997–10003, 2015. <https://doi.org/10.1039/c4cp05666c>.
- [47] J. Li, Z. L. Zhang, L. Du, et al., “Highly stable femtosecond pulse generation from a MXene $\text{Ti}_3\text{C}_2\text{T}_x$ (T = F, O, or OH) mode-locked fiber laser,” *Photon. Res.*, vol. 7, pp. 260–264, 2019. <https://doi.org/10.1364/PRJ.7.000260>.
- [48] Q. Wu, X. Jinn, S. Chen, et al., “MXene-based saturable absorber for femtosecond mode-locked fiber lasers,” *Opt. Express*, vol. 27, pp. 10159–10170, 2019. <https://doi.org/10.1364/OE.27.010159>.
- [49] J. Yi, L. Du, J. Li, et al., “Unleashing the potential of Ti_2CT_x MXene as a pulse modulator for mid-infrared fiber lasers,” *2D Mater.*, vol. 6, 2019, Art no. 045038. <https://doi.org/10.1088/2053-1583/ab39bc>.
- [50] L. E. Nelson, D. J. Jones, K. Tamura, H. A. Haus, and E. P. Ippen, “Ultrashort-pulse fiber ring lasers,” *Appl. Phys. B*, vol. 65, pp. 277–294, 1997. <https://doi.org/10.1007/s003400050273>.
- [51] Q. Bao, H. Zhang, Z. Ni, et al., “Monolayer graphene as a saturable absorber in a mode-locked laser,” *Nano Res.*, vol. 4, pp. 297–307, 2010. <https://doi.org/10.1007/s12274-010-0082-9>.
- [52] D. Mao, B. Jiang, X. Gan, et al., “Soliton fiber laser mode locked with two types of film-based Bi_2Te_3 saturable absorbers,” *Photonics Res.*, vol. 3, 2015. <https://doi.org/10.1364/PRJ.3.000A43>.
- [53] Z. Luo, Y. Li, M. Zhong, et al., “Nonlinear optical absorption of few-layer molybdenum diselenide (MoSe_2) for passively mode-locked soliton fiber laser [Invited],” *Photon. Res.*, vol. 3, 2015. <https://doi.org/10.1364/PRJ.3.000A79>.
- [54] Y. Chen, G. Jiang, S. Chen, et al., “Mechanically exfoliated black phosphorus as a new saturable absorber for both Q-switching and mode-locking laser operation,” *Opt. Express*, vol. 23, pp. 12823–12833, 2015. <https://doi.org/10.1364/OE.23.012823>.
- [55] K. Krupa, K. Nithyanandan, U. Andral, P. Tchofo-Dinda, and P. Grelu, “Real-time observation of internal motion within ultrafast dissipative optical soliton molecules,” *Phys. Rev. Lett.*, vol. 118, p. 243901, 2017. <https://doi.org/10.1103/PhysRevLett.118.243901>.
- [56] X. Li, Y. Wang, W. Zhang, and W. Zhao, “Experimental observation of soliton molecule evolution in Yb-doped passively mode-locked fiber lasers,” *Laser Phys. Lett.*, vol. 11, 2014, Art no. 075103. <https://doi.org/10.1088/1612-2011/11/7/075103>.